REPORT

Synaptotagmin 2 Mutations Cause an Autosomal-Dominant Form of Lambert-Eaton Myasthenic Syndrome and Nonprogressive Motor Neuropathy

David N. Herrmann,[1,8] Rita Horvath,[2,8] Janet E. Sowden,[1] Michael Gonzales,[3] Avencia Sanchez-Mejias,[3] Zhuo Guan,[4] Roger G. Whittaker,[5] Jorge L. Almodovar,[6] Maria Lane,[2] Boglarka Bansagi,[2] Angela Pyle,[2] Veronika Boczonadi,[2] Hanns Lochmüller,[2] Helen Griffin,[2] Patrick F. Chinnery,[2] Thomas E. Lloyd,[7] J. Troy Littleton,[4,8] and Stephan Zuchner[3,8,*]

Synaptotagmin 2 is a synaptic vesicle protein that functions as a calcium sensor for neurotransmission but has not been previously associated with human disease. Via whole-exome sequencing, we identified heterozygous missense mutations in the C2B calcium-binding domain of the gene encoding Synaptotagmin 2 in two multigenerational families presenting with peripheral motor neuron syndromes. An essential calcium-binding aspartate residue, Asp307Ala, was disrupted by a c.920A>C change in one family that presented with an autosomal-dominant presynaptic neuromuscular junction disorder resembling Lambert-Eaton myasthenic syndrome. A c.923C>T variant affecting an adjacent residue (p.Pro308Leu) produced a presynaptic neuromuscular junction defect and a dominant hereditary motor neuropathy in a second family. Characterization of the mutation homologous to the human c.920A>C variant in *Drosophila* Synaptotagmin revealed a dominant disruption of synaptic vesicle exocytosis using this transgenic model. These findings indicate that Synaptotagmin 2 regulates neurotransmitter release at human peripheral motor nerve terminals. In addition, mutations in the Synaptotagmin 2 C2B domain represent an important cause of presynaptic congenital myasthenic syndromes and link them with hereditary motor axonopathies.

Synaptotagmin 2 (SYT2), a synaptic vesicle protein, is the major isoform of the synaptotagmin family at mammalian neuromuscular junctions (NMJs) and functions as a calcium sensor for neurotransmission.[1,2] The C2B domain of SYT2 is essential for neurotransmitter release at the NMJ in several animal models, although mutations in *SYT2* (MIM 600104) have not been previously linked to human disease.[1,3] Here we describe two multigenerational families with dominant mutations of adjacent residues in the SYT2 C2B domain that cause a disorder with features including presynaptic NMJ dysfunction resembling Lambert-Eaton myasthenic syndrome (LEMS) and motor neuropathy. We model and validate the identified dominant defects of the protein in a *Drosophila* model that recapitulates key synaptic dysfunctions found in affected individuals.

In the three-generational index family USA1, affected family members developed foot deformities in childhood including pes cavus and hammer toes (Figure 1). These individuals had a variable degree of proximal and distal limb weakness, muscle fatigue that improved with rest, mild gait difficulties, and reduced or absent deep tendon reflexes that could be elicited after brief exercise. Acetylcholine receptor binding, blocking and modulating antibodies, and voltage-gated calcium channel antibodies were negative in the proband in USA1. In a second family (UK1), affected individuals (Figure 1) also presented with childhood-onset foot deformities, but had congenital hip dislocation (in affected females), distal, often asymmetric lower extremity muscle atrophy, lower limb predominant weakness, and absent deep tendon reflexes. A summary of the clinical features of each person in both families is included in Table 1. Electrophysiological studies in USA1 (Figure 2, Table S1 available online) showed presynaptic NMJ dysfunction with low-amplitude compound muscle potentials (CMAPs) and marked CMAP amplitude increments after brief exercise. Concentric needle electromyography was normal in weak muscles in affected USA1 family members. In UK1, electrophysiologic abnormalities included low-amplitude lower-limb CMAPs with a variable degree of postexercise amplitude facilitation and slight reinnervation on needle electromyography of distal muscles, consistent with motor neuropathy (Figure 2, Table S2). Sensory nerve conduction studies were normal in all individuals in each family (Tables S1 and S2).

A whole-exome sequencing study was undertaken in each family, under Institutional Review Board approval, and after written informed consent. Whole-exome sequencing in USA1 family members II.2, III.2, and II.1 (unaffected) was performed with the 50Mbases Agilent

[1]Department of Neurology, University of Rochester Medical Center, Rochester, NY 14642, USA; [2]Institute of Genetic Medicine, Newcastle University, Newcastle upon Tyne NE1 3BZ, UK; [3]Dr. John T. Macdonald Foundation, Department of Human Genetics and John P. Hussman Institute for Human Genomics, University of Miami Miller School of Medicine, Miami, FL 33136, USA; [4]The Picower Institute for Learning and Memory, Department of Biology and Department of Brain and Cognitive Sciences, Massachusetts Institute of Technology, Cambridge, MA 02139, USA; [5]Institute of Neuroscience, Newcastle University, Newcastle upon Tyne NE2 4HH, UK; [6]Department of Neurology, Dartmouth Hitchcock Clinic, Geisel School of Medicine, Hanover, NH 03755, USA; [7]Departments of Neurology and Neuroscience, Johns Hopkins University School of Medicine, Baltimore, MD 21205, USA
[8]These authors contributed equally to this work
*Correspondence: szuchner@med.miami.edu
http://dx.doi.org/10.1016/j.ajhg.2014.08.007.

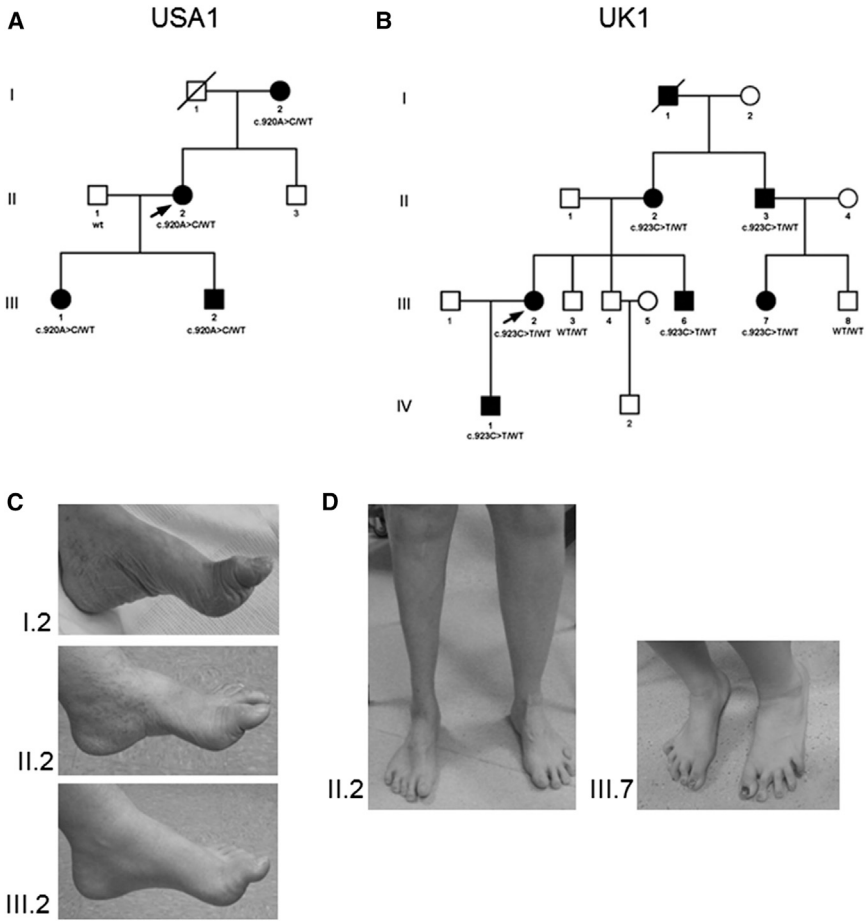

Figure 1. Pedigrees of Affected Families and Lower Limb Deformities
(A and B) Family pedigrees for USA1 (A) and UK1 (B). Filled symbols are clinically affected individuals, arrows denote the probands.
(C) Foot and toe deformities in three generations in the USA1 family.
(D) Asymmetric distal lower limb muscle atrophy (individual II.2 shown here) was noted in affected UK1 females. Splayed toes (family member III.7) were notable in the UK1 kindred.

SureSelect v.4 capture kit combined with an Illumina HiSeq2000 sequencing instrument. Raw data were aligned with the BWA software and variants were called using GATK. All resulting variants and also genotype calls at non-variant positions were annotated, and segregation patterns were calculated with the GEDI protocol.[4] After import into the GEM.app software, we filtered for dominantly segregating variants and excluded variants that were present in the NHLBI EVS data set of 6,500 individuals, the local GEM.app data set of 3,000 individuals, variants with GERP conservation scores of less than 3, and genes with a residual variation intolerance score of >95 percentile.[5] We considered only nonsynonymous variants, splice site changes, and indels. Using five different protein prediction algorithms (Polyphen, MutationTaster, MutationAssessor, SIFT, LRT), we created a composite score where each "damaging" assessment receives one point. Of the six remaining genes from this analysis, only one gene, *SYT2*, had a full score of 5 (Table S3). Full Sanger-based segregation analysis of all six genes in the USA1 family reduced the gene list to only two candidates, including a heterozygous c.920A>C (p.Asp307Ala) missense mutation (RefSeq accession number NM_177402.4) in the gene encoding SYT2 (Figure 2, Table S3). *SYT2* represents an enticing candidate given its well-established role in calcium activation of neurotransmitter release at NMJs.[1–3] Further, Asp307, an aspartate residue, is the second of five residues that coordinate calcium binding to the C2B domain (Figure 2).[6] Disruption of these residues leads to a loss of calcium binding and dominant-negative disruption of exocytosis in *Drosophila*.[7–10]

Whole-exome sequencing in family UK1 (individuals III:2 and IV:1) was performed with the Illumina TruSeq 62 Mb exome capture and sequenced on an Illumina HiSeq 2000 instrument. The in-house bioinformatics pipeline at Newcastle University included alignment to the human reference genome (UCSC hg19), reformatting, and variant detection (Varscan v.2.2, Dindel v.1.01), as described previously.[11] On-target variant filtering excluded those with minor allele frequency greater than 0.01 in several databases. Rare homozygous and compound heterozygous variants were defined, and protein altering and/or putative "disease-causing" mutations, along with their functional annotation, were identified using ANNOVAR. Lists of on-target ariants were filtered against data from NHLBI-6500-ESP, the 1000 Genomes project, and the exome sequences of 334 unrelated in-house control exomes to identify rare homozygous variants with a MAF < 0.01. Putative pathogenic variants were confirmed by Sanger sequencing and segregation analyses was performed. This sequencing revealed a heterozygous segregating missense mutation affecting the amino acid residue adjacent to USA1 (c.923C>T [p.Pro308Leu]) (Figure 2). This change was also predicted to be deleterious and not present in controls. No other segregating variants were identified in this family (Table S3).

To determine how these *SYT2* mutations might alter synaptic function, we focused on the c.920A>C (p.Asp307Ala) variant given its established role in calcium binding to the C2B domain. We generated transgenic *Drosophila* containing wild-type (WT) and mutant Synaptotagmin genes using the GAL4-UAS expression system. *Drosophila* contains a single isoform (DSYT1) of the

Table 1. Clinical Features in Family Members in USA1 and UK1 Affected by *SYT2* Mutations

	USA1 (c.920A>C [p.Asp307Ala])				UK1 (c.923C>T [p.Pro308Leu])					
	I.2	**II.2**[a]	**III.1**	**III.2**	**II.2**	**II.3**	**III.2**[a]	**III.6**	**III.7**	**IV.1**
Age (years)	70	49	23	15	44	42	27	16	12	7
Gender	F	F	F	M	F	M	F	M	F	M
Foot or Toe Deformity, Joint Abnormalities[b]										
Feet/Toes	C,H	C,H,S	C,H	C,H	C,S	H	HA,H	C,H	C,H,S	P
Hip dysplasia	–	–	–	–	+	–	+	–	+	–
Lower Limb Features[c]										
Weakness	P = D	P = D,F	–	–	R > L; R: D,P; L: D	D	D	–	R > L,D	–
Wasting	–	–	–	–	R: D,P; L: D	D	D	–	–	–
Tendon reflexes	A	A,F	A, Red	A,F	A	A,F	A	A	A	A
Upper Limb Features[c]										
Weakness	D	p = D,F	–	–	D	–	D	–	–	–
Tendon reflexes	A	A,F	A,F	A,F	A	A	A	A	A	A
Motor Development and Gait[d]										
Delayed milestones	–	–	–	–	–	–	–	–	–	+
Rapid fatigue with activity	–	++	–	+	–	–	–	–	–	–
Gait abnormalities	W	TW, HW	–	+	W, HW, TW	HW, TW	W, HW, TW	–	HW	W, HW
Orthotics	–	–	–	–	KO	–	AFO	–	–	FO
Orthopedic surgeries	–	T	–	–	K,F	A,T	F	–	–	–
Difficulty with sports	–	+	–	+	+	–	+	+	–	+
Other Clinical Findings										
Hearing loss	+	+	–	–	–	–	–	–	–	–
Benign positional vertigo	–	+	–	–	–	–	–	–	–	–
Sensory loss (hands or feet)	–	–	–	–	+	–	+	–	–	+
Electrophysiological Findings[e]										
CMAP amplitudes	Red	Red	Red	Red	Red	Red	Red	N	Red	ND
CMAP facilitation	-	+++	+++	+++	-	+	+++	ND	++	ND
SNAP amplitudes	N	N	N	N	N	N	N	N	N	N
EMG	N	N	ND	ND	R	R	R	R	R	ND

[a]Proband
[b]Abbreviations are as follows: C, pes cavus; P, pes planus; HA, high arch; H, hammer toes; S, splayed toes.
[c]Abbreviations are as follows: P, proximal; D, distal; R, right; L, left; A, absent; N, normal; ND, not done; F, facilitation with exercise; Red, reduced. Minus sign (–) indicates not present; plus sign (+) indicates present.
[d]Abbreviations are as follows: AFO, ankle foot orthotic; FO, foot orthotics; KO, knee orthotic; K, knee surgery; A, ankle surgery; F, foot surgery; T, toe surgery; W, waddling gait; HW, unable/impaired heel walk; TW, impaired toe walk. Minus sign (–) indicates not present; plus sign (+) indicates present.
[e]See Tables S2 and S3 for detailed electrophysiologic findings. Facilitation denotes an increase in tendon reflexes, strength, or CMAP amplitude after 10 s of maximal voluntary contraction. USA II.1, a 49-year-old male and the husband of the proband, UK III.3 (a 24-year-old male and brother of the proband), and UK III.8 (a 9-year-old female cousin of the proband) are unaffected with no neurologic symptoms or signs and no foot deformities. Abbreviations are as follows: CMAP, compound muscle action potential; Red, reduced; SNAP, sensory nerve action potential; EMG, needle electromyography; R, reinnervation; N, normal; ND, not done. Single plus sign (+) indicates 30%–49% CMAP amplitude increase after 10 s of exercise; double plus sign (++) indicates 50%–99% CMAP amplitude increase; triple plus sign (+++) indicates >100% CMAP amplitude increase.

mammalian synaptic vesicle SYT subfamily (SYT1, SYT2, SYT9). DSYT1 is highly homologous to human SYT2, with perfect conservation of the five C2B calcium binding residues, including Asp307 (corresponding to Asp362 in *Drosophila*) (Figure 3A, Figure S1). We generated transgenic WT and c.1527A>C (p.Asp362Ala) *UAS-DSyt1* lines and induced these genes using the pan neuronal GAL4 driver elav^{C155} (Figures 3B and 3C). The p.Asp362Ala protein localized normally to synapses in both the *syt1*$^{-/-}$ null and wild-type backgrounds (Figure 3C). Neurotransmitter release was analyzed at third instar *Drosophila* NMJs using current recordings of postsynaptic responses in voltage

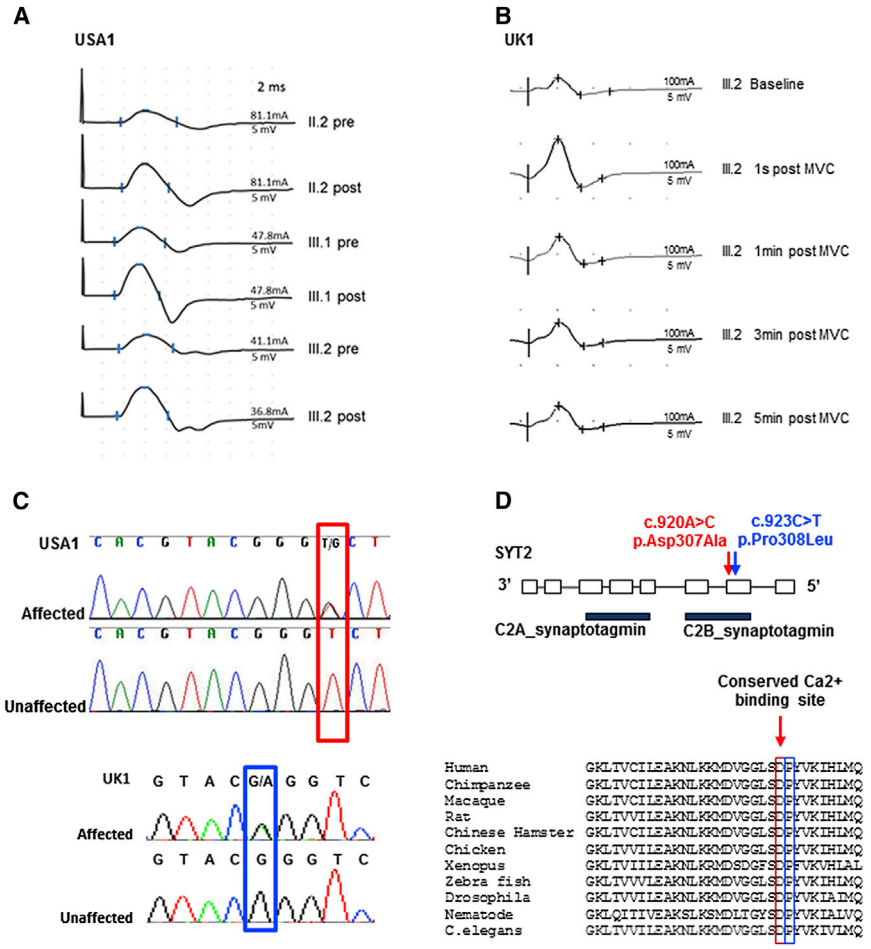

Figure 2. Postexercise Compound Muscle Action Potential Amplitude Facilitation in USA1 and UK1 and Family Genetic Studies

(A) Median nerve distal CMAP before and immediately after 10 s of maximal voluntary contraction for USA1 proband II.2 and her affected offspring III.1 and III.2. Each of these individuals demonstrated a greater than 100% increment in median nerve distal compound muscle action potential amplitude following brief exercise. Individual II.2 also demonstrated a 139% increment in the peroneal motor distal compound muscle action potential amplitude recording from the tibialis anterior muscle. Individuals III.1 and III.2 additionally demonstrated 110% and 200% distal ulnar compound muscle action potential amplitude increments, respectively, after 10 s of exercise. See Table S1 for full electrophysiological data for USA1.

(B) Amplitude and area increment of the peroneal CMAP (recording from tibialis anterior) in the UK1 proband (III.2) after 10 s of maximal voluntary contraction (MVC), which persisted beyond 5 min. See Table S2 for electrophysiologic data for UK1.

(C) Sanger traces demonstrating the c.920A>C missense mutation in *SYT2* in USA1. This produces an amino acid change from aspartate to alanine at the second aspartate residue (p.Asp307Ala) in the cytoplasmic C2B domain of SYT2. A c.923C>T missense mutation in *SYT2* in affected UK1 individuals results in a proline-to-leucine amino acid change at the adjacent residue (p.Pro308Leu). Note that the *SYT2* gene is encoded at the opposite strand.

(D) Position of the identified mutations in each family on the gene structure of *SYT2* and the conservation of the affected residues across species.

clamp. p.Asp362Ala failed to rescue any of the defects observed in the *DSyt1*-null background (Figures 3D–3H). Rescued animals with p.Asp362Ala DSYT1 lacked synchronous neurotransmitter release and displayed enhanced asynchronous release and elevated spontaneous fusion rates as previously described in *DSyt1*-null mutants.[8,10] These results indicate that the p.Asp362Ala mutation completely abolishes the ability of the protein to support calcium-triggered neurotransmitter release.

We next assayed the effects of the p.Asp362Ala protein on synaptic transmission in the presence of endogenous DSYT1, mimicking the dominant human condition. Four independent transgenic p.Asp362Ala lines were lethal when driven with the pan neuronal GAL4 driver elav^{C155} in *Drosophila* neurons. Two transgenic lines, C2B#1 (with induced levels of p.Asp362Ala protein similar to WT DSYT1) (Figure 3B) and C2B#2 (induced at a slightly higher level), were further characterized. Induction of p.Asp362Ala DSYT1 in the presence of endogenous DSYT1 caused a striking dominant-negative effect on neuromuscular transmission, while WT DSYT1 had no effect (Figures 4, S2, and S3). p.Asp362Ala induction reduced evoked release (Figures 4A and 4B) and increased the frequency of spontaneous fusion events (Figures 4C and 4D). The p.Asp362Ala C2B#2 transgenic line produced a more severe phenotype, indicating dosage-dependent disruptions in synaptic transmission. High-frequency stimulation revealed increased facilitation of evoked release in the presence of p.Asp362Ala (Figures 4E and 4F), consistent with a reduction in initial release probability caused by the mutant protein and similar to the observation of enhanced CMAP amplitude after exercise in the USA1 family. These findings indicate that the SYT mutant exerts a strong dominant-negative effect on synaptic transmission that mimics many aspects of the defects observed at the NMJs of affected USA1 family members.

How does the SYT2 mutant protein dominantly interfere with neurotransmitter release? We previously demonstrated that SYT functions as a multimer in vivo in *Drosophila*, consistent with structural studies of the protein.[9,12,13] The dominant effect observed in the c.920A>C family and the phenotypes of p.Asp362Ala in *Drosophila* suggest that mutant SYT2 is likely to multimerize with endogenous SYT2 and disrupt its normal properties, resulting in the defects in synaptic transmission we observe in both systems. Synaptotagmins have been

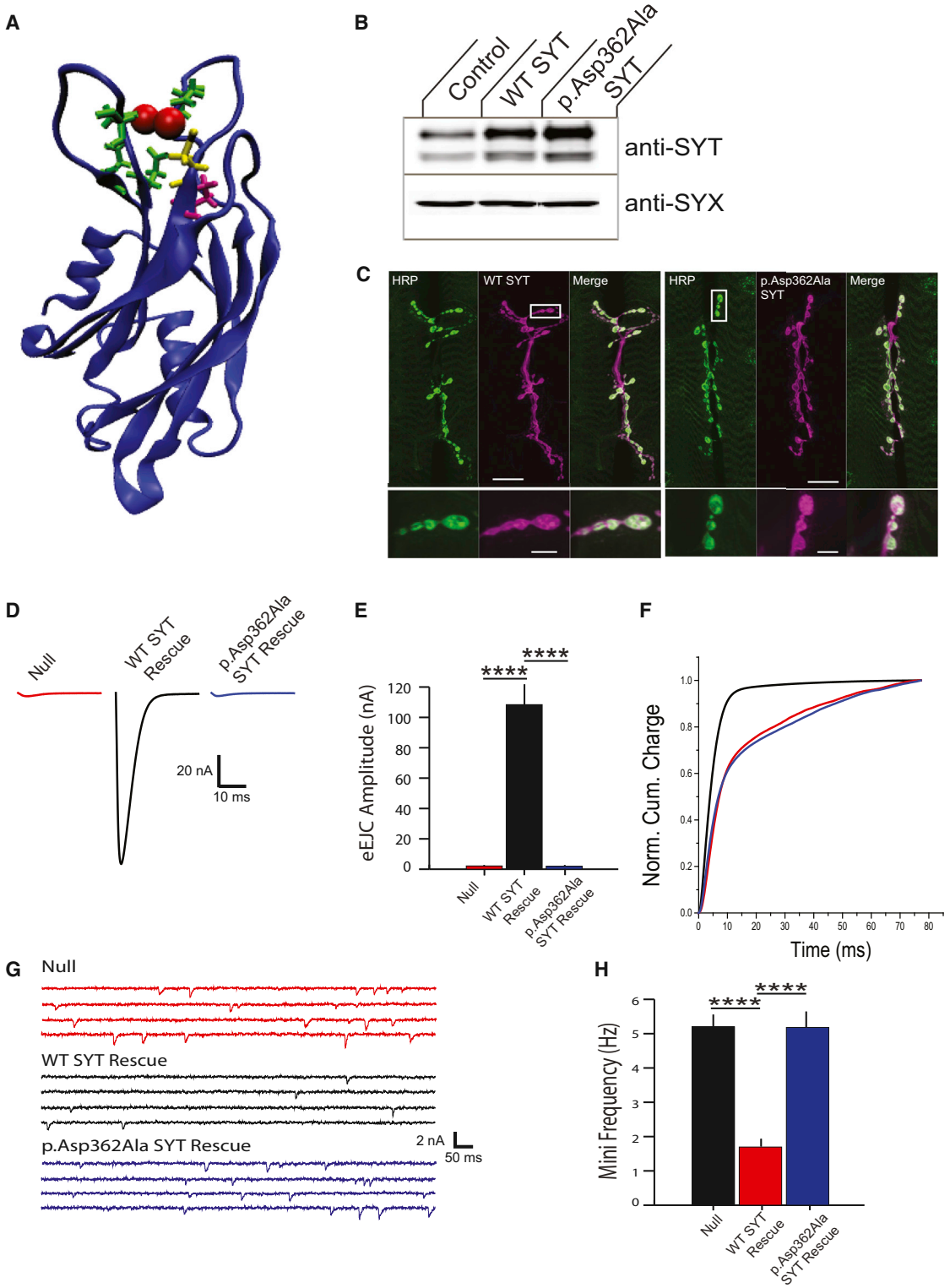

Figure 3. p.Asp362Ala DSYT1 Fails to Support Neurotransmitter Release in a *synaptotagmin*-Null Mutant

(A) Stereoview of the Asp307 (yellow) and Pro308 (magenta) residues modeled on the rat SYT1 C2B crystal structure. The five essential Ca^{2+}-binding residues are highlighted in green and Ca^{2+} ions in red.

(B) Immunoblot with anti-SYT (top) or anti-Syntaxin (SYX; control) antisera from head extracts of control or transgenic *Drosophila* following wild-type (WT) or p.Asp362Ala DSYT induction by $elav^{C155}$-GAL4.

(C) Representative larval NMJs stained with anti-Myc antisera (green) for animals with Myc-tagged WT or p.Asp362Ala SYT1. The axon is stained with the neuronal marker anti-HRP (magenta). The boxed area is magnified in the bottom panel. Mutant SYT1 targets normally to presynaptic terminals. Scale bars represent 20 μM (top) or 5 μM (bottom).

(D) Representative EPSCs recorded in 2 mM external Ca^{2+} in $Dsyt1^{-/-}$ null larvae (red) and null mutants rescued with WT DSYT1 (black) or p.Asp362Ala DSYT1 (blue).

(legend continued on next page)

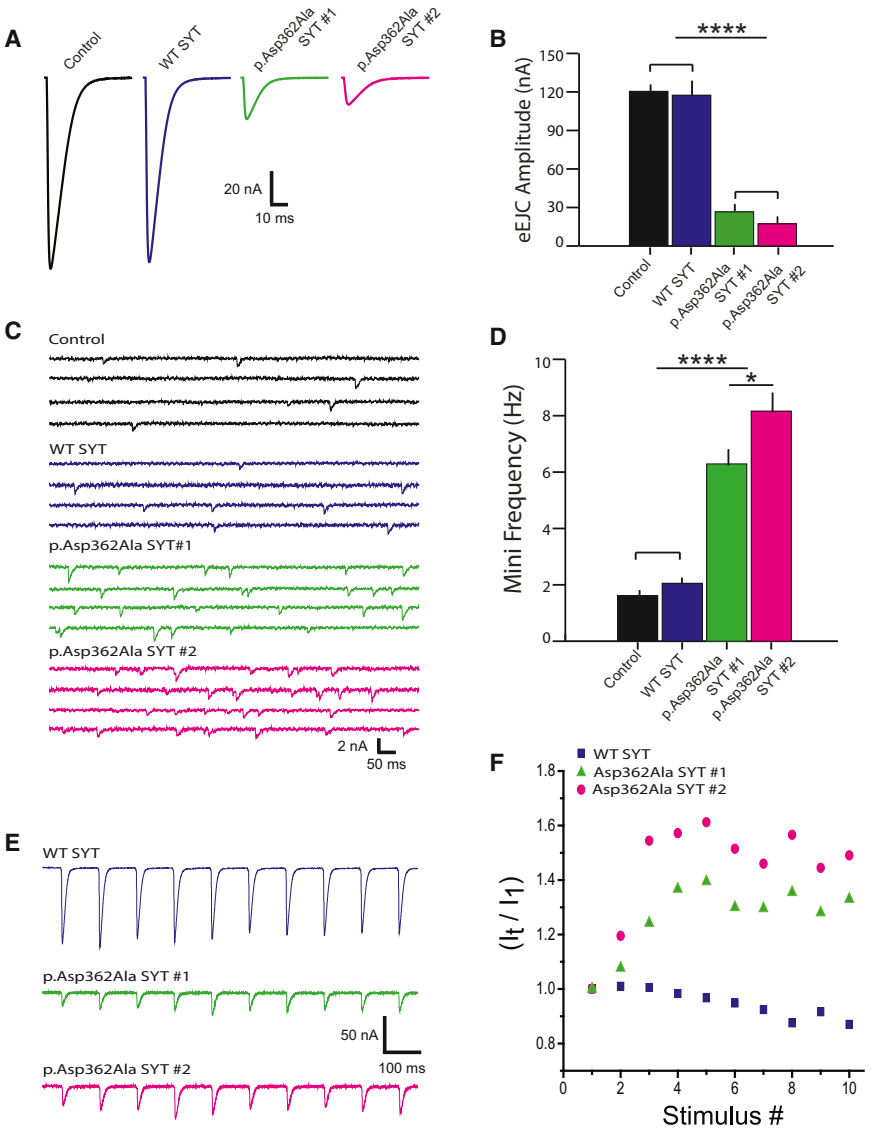

Figure 4. Mutant Synaptotagmin Disrupts Neurotransmitter Release in the Presence of Endogenous Synaptotagmin

(A) Representative EPSCs recorded in 0.2 mM extracellular Ca^{2+} at third instar larval muscle 6 synapses for the indicated genotypes (control, induction of WT or p.Asp362Ala DSYT1 by elav^{C155}-GAL4).

(B) Quantification of mean eEJC amplitudes in the indicated genotypes ($w^{-/-}$, 120.5 ± 5.3 nA, n = 16; elav^{C155}-GAL4; UAS-SYT1, 117.5 ± 11 nA, n = 15; elav^{C155}-GAL4; UAS-SYT1 p.Asp362Ala#1, 26.6 ± 4.7 nA, n = 16; elav^{C155}-GAL4; UAS-SYT1 p.Asp362Ala#2, 17.3 ± 3.2 nA, n = 16).

(C) Postsynaptic current recordings of spontaneous release for the indicated genotypes.

(D) Quantification of average mini frequency for the indicated genotypes ($w^{-/-}$, 1.6 ± 0.1 Hz, n = 10; elav^{C155}-GAL4; UAS-SYT1, 2.1 ± 0.2 Hz, n = 10; elav^{C155}-GAL4; UAS-SYT1 p.Asp362Ala#1, 6.3 ± 0.5 Hz, n = 16; elav^{C155}-GAL4; UAS-SYT1 p.Asp362Ala#2, 8.2 ± 0.7 Hz, n = 13). Student's t test: *p < 0.05; ****p < 0.0001. Error bars represent SEM.

(E) Representative EPSCs during a short 10 Hz tetanic stimulation of the nerve in 0.2 mM external Ca^{2+} for the indicated genotypes.

(F) The average for the first ten responses normalized to the first response during the tetanus is shown following induction of WT DSYT 1 (blue), DSYT1 p.Asp362Ala #1 (green), and DSYT1 p.Asp362Ala #2 (red). The average fast tetanic facilitation after ten responses for each genotype is: WT DSYT1 = 0.94 ± 0.02; DSYT1 p.Asp362Ala#1 = 1.29 ± 0.03; DSYT1 p.Asp362Ala#2 = 1.49 ± 0.04. Student's t test revealed significant differences between WT and p.Asp362Ala (p < 0.0001).

suggested to function as fusion clamps to prevent spontaneous exocytosis, in addition to their role as calcium sensors for evoked release, which likely explains why spontaneous fusion is increased in the *Drosophila* model.[1,2] We postulate that the SYT2 p.Pro308Leu residue will alter calcium binding to the C2B domain as well.

While the clinical presentation in the two families shows similarities, including foot deformity, areflexia, and limb weakness, there are also features with variable degrees of penetrance. In family USA1, harboring the c.920A>C (p.Asp307Ala) variant, three of four individuals (II.2, III.1, and III.2) showed a pure presynaptic NMJ disorder with low-amplitude CMAPs and a marked postexercise increment of CMAP amplitude. Intriguingly, this resembles findings in an autoimmune-induced clinical form of presynaptic dysfunction called Lambert-Eaton myasthenic syndrome.[14] In this rare condition, antibodies target presynaptic voltage-gated calcium channels, but

(E) Quantification of mean excitatory junctional current (eEJC) amplitudes in the indicated genotypes (*Dsyt1*$^{-/-}$ null, 2.1 ± 0.3 nA, n = 10; elav^{C155}-GAL4; *Dsyt1*$^{-/-}$; UAS-SYT1, 108.4 ± 13.9 nA, n = 18; elav^{C155}-GAL4; *Dsyt1*$^{-/-}$; UAS-SYT1 p.Asp362Ala, 2.0 ± 0.5 nA, n = 13).

(F) Cumulative vesicle release defined by charge transfer normalized for the maximum in 2.0 mM Ca^{2+} for each genotype (same color code as in D). Each trace was adjusted to a double exponential fit. Both the null and p.Asp362Ala rescued animals display a prominent increase in the slow asynchronous phase of release.

(G) Postsynaptic current recordings of spontaneous release at muscle 6 synapses in *Dsyt1*$^{-/-}$ null larvae (red) and null mutants rescued with WT DSYT1 (black) or p.Asp362Ala DSYT1 (blue).

(H) Quantification of mini frequency in the indicated genotypes (*Dsyt1*$^{-/-}$ null, 5.2 ± 0.6 Hz, n = 8; elav^{C155}-GAL4; *Dsyt1*$^{-/-}$; UAS-SYT1, 1.7 ± 0.2 Hz, n = 16; elav^{C155}-GAL4; *Dsyt1*$^{-/-}$; UAS-SYT1 p.Asp362Ala, 5.2 ± 0.4 Hz, n = 12).
Student's t test: ****p < 0.0001. Error bars represent SEM.

antibodies against synaptotagmins have also been identified in some individuals.[15] Family members from UK1, harboring the c.923C>T (p.Pro308Leu) variant, also had low-amplitude CMAPs, but only one person (III.2) exhibited marked, postexercise CMAP amplitude increments that were longer lasting than in individuals from USA1. Some UK1 individuals also had muscle wasting, and needle electromyography disclosed mild chronic distal muscle reinnervation. Mutation in the presynaptic choline transporter has also been shown to cause a lower motor neuron phenotype, suggesting that presynaptic dysfunction may be a more general mechanism for peripheral axonopathies.[16] *SYT2* is also expressed in other tissues outside of the NMJ, including the cerebellum and cochlea. Analysis of additional families will be necessary to define the spectrum of human phenotypes associated with *SYT2* mutations.

In summary, mutations in the *SYT2* C2B domain represent an important cause of disorders of the human peripheral motor nerve terminal; foot deformities are a hallmark, with phenotypes ranging from a dominant NMJ syndrome resembling Lambert-Eaton myasthenic syndrome to mixed manifestations of distal hereditary motor neuropathy and presynaptic NMJ dysfunction.

Supplemental Data

Supplemental Data include three figures and three tables and can be found with this article online at http://dx.doi.org/10.1016/j.ajhg.2014.08.007.

Acknowledgments

D.N.H. and J.E.S. are supported by the Inherited Neuropathies Consortium Rare Disease Clinical Research Network, National Institute of Neurological Disorders and Stroke (1U54NS0657); J.T.L. and Z.G. are supported by NIH grant NS40296, the Picower Neurological Disease Research Fund, and The JPB Foundation; T.E.L. is supported by NIH grant NS082563; S.Z., A.S.-M., and M.G. are supported by NIH grants U54NS0657, R01NS075764, R01NS072248, the MDA, and the CMT Association; R.H. is supported by the Medical Research Council (UK) (G1000848) and the European Research Council (309548); R.G.W. is supported by the EPSRC and the Wellcome Trust; B.B. is supported by the Medical Research Council Neuromuscular Translational Research Centre; H.L. receives funding from the European Union Seventh Framework Programme (FP7/2007-2013) under grant agreement No. 305444 (RD-Connect) and 305121 (Neuromics); and P.F.C. is a Wellcome Trust Senior Fellow in Clinical Science (101876/Z/13/Z) and a UK NIHR Senior Investigator and receives additional support from the Wellcome Trust Centre for Mitochondrial Research (096919Z/11/Z), the Medical Research Council (UK) Centre for Translational Muscle Disease research (G0601943), EU FP7 TIRCON, and the National Institute for Health Research (NIHR) Newcastle Biomedical Research Centre based at Newcastle upon Tyne Hospitals NHS Foundation Trust and Newcastle University. The views expressed are those of the author(s) and not necessarily those of the NHS, the NIHR, or the Department of Health. The authors would like to thank Eric Logigian for electrophysiological advice and Tracy Forrester for administrative assistance with manuscript preparation.

Received: July 16, 2014
Accepted: August 15, 2014
Published: September 4, 2014

Web Resources

The URLs for data presented herein are as follows:

1000 Genomes, http://browser.1000genomes.org
ANNOVAR, http://www.openbioinformatics.org/annovar/
GEM.app, https://genomics.med.miami.edu
Mutation Assessor, http://mutationassessor.org/
MutationTaster, http://www.mutationtaster.org/
NHLBI Exome Sequencing Project (ESP) Exome Variant Server, http://evs.gs.washington.edu/EVS/
Online Mendelian Inheritance in Man (OMIM), http://www.omim.org/
PolyPhen-2, http://www.genetics.bwh.harvard.edu/pph2/
SIFT, http://sift.bii.a-star.edu.sg/
UCSC Genome Browser, http://genome.ucsc.edu

References

1. Pang, Z.P., Melicoff, E., Padgett, D., Liu, Y., Teich, A.F., Dickey, B.F., Lin, W., Adachi, R., and Südhof, T.C. (2006). Synaptotagmin-2 is essential for survival and contributes to Ca2+ triggering of neurotransmitter release in central and neuromuscular synapses. J. Neurosci. *26*, 13493–13504.
2. Littleton, J.T., Stern, M., Schulze, K., Perin, M., and Bellen, H.J. (1993). Mutational analysis of *Drosophila* synaptotagmin demonstrates its essential role in Ca(2+)-activated neurotransmitter release. Cell *74*, 1125–1134.
3. Wen, H., Linhoff, M.W., McGinley, M.J., Li, G.L., Corson, G.M., Mandel, G., and Brehm, P. (2010). Distinct roles for two synaptotagmin isoforms in synchronous and asynchronous transmitter release at zebrafish neuromuscular junction. Proc. Natl. Acad. Sci. USA *107*, 13906–13911.
4. Gonzalez, M.A., Lebrigio, R.F., Van Booven, D., Ulloa, R.H., Powell, E., Speziani, F., Tekin, M., Schüle, R., and Züchner, S. (2013). GEnomes Management Application (GEM.app): a new software tool for large-scale collaborative genome analysis. Hum. Mutat. *34*, 842–846.
5. Petrovski, S., Wang, Q., Heinzen, E.L., Allen, A.S., and Goldstein, D.B. (2013). Genic intolerance to functional variation and the interpretation of personal genomes. PLoS Genet. *9*, e1003709.
6. Sutton, R.B., Davletov, B.A., Berghuis, A.M., Südhof, T.C., and Sprang, S.R. (1995). Structure of the first C2 domain of synaptotagmin I: a novel Ca2+/phospholipid-binding fold. Cell *80*, 929–938.
7. Mackler, J.M., Drummond, J.A., Loewen, C.A., Robinson, I.M., and Reist, N.E. (2002). The C(2)B Ca(2+)-binding motif of synaptotagmin is required for synaptic transmission in vivo. Nature *418*, 340–344.
8. Yoshihara, M., and Littleton, J.T. (2002). Synaptotagmin I functions as a calcium sensor to synchronize neurotransmitter release. Neuron *36*, 897–908.
9. Lee, J., Guan, Z., Akbergenova, Y., and Littleton, J.T. (2013). Genetic analysis of synaptotagmin C2 domain specificity in

regulating spontaneous and evoked neurotransmitter release. J. Neurosci. *33*, 187–200.

10. Jorquera, R.A., Huntwork-Rodriguez, S., Akbergenova, Y., Cho, R.W., and Littleton, J.T. (2012). Complexin controls spontaneous and evoked neurotransmitter release by regulating the timing and properties of synaptotagmin activity. J. Neurosci. *32*, 18234–18245.
11. Pfeffer, G., Elliott, H.R., Griffin, H., Barresi, R., Miller, J., Marsh, J., Evilä, A., Vihola, A., Hackman, P., Straub, V., et al. (2012). Titin mutation segregates with hereditary myopathy with early respiratory failure. Brain *135*, 1695–1713.
12. Littleton, J.T., Stern, M., Perin, M., and Bellen, H.J. (1994). Calcium dependence of neurotransmitter release and rate of spontaneous vesicle fusions are altered in *Drosophila* synaptotagmin mutants. Proc. Natl. Acad. Sci. USA *91*, 10888–10892.
13. Wu, Y., He, Y., Bai, J., Ji, S.R., Tucker, W.C., Chapman, E.R., and Sui, S.F. (2003). Visualization of synaptotagmin I oligomers assembled onto lipid monolayers. Proc. Natl. Acad. Sci. USA *100*, 2082–2087.
14. Titulaer, M.J., Lang, B., and Verschuuren, J.J. (2011). Lambert-Eaton myasthenic syndrome: from clinical characteristics to therapeutic strategies. Lancet Neurol. *10*, 1098–1107.
15. Takamori, M., Maruta, T., and Komai, K. (2000). Lambert-Eaton myasthenic syndrome as an autoimmune calcium-channelopathy. Neurosci. Res. *36*, 183–191.
16. Barwick, K.E., Wright, J., Al-Turki, S., McEntagart, M.M., Nair, A., Chioza, B., Al-Memar, A., Modarres, H., Reilly, M.M., Dick, K.J., et al. (2012). Defective presynaptic choline transport underlies hereditary motor neuropathy. Am. J. Hum. Genet. *91*, 1103–1107.

The American Journal of Human Genetics, Volume *95*

Supplemental Data

Synaptotagmin 2 Mutations Cause Autosomal-Dominant Form of Lambert-Eaton Myasthenic Syndrome and Nonprogressive Motor Neuropathy

David N. Herrmann, Rita Horvath, Janet E. Sowden, Michael Gonzales, Avencia Sanchez-Mejias, Zhuo Guan, Roger G. Whittaker, Jorge L. Almodovar, Maria Lane, Boglarka Bansagi, Angela Pyle, Veronika Boczonadi, Hanns Lochmüller, Helen Griffin, Patrick F. Chinnery, Thomas E. Lloyd, J. Troy Littleton, and Stephan Zuchner

Figure S1

A

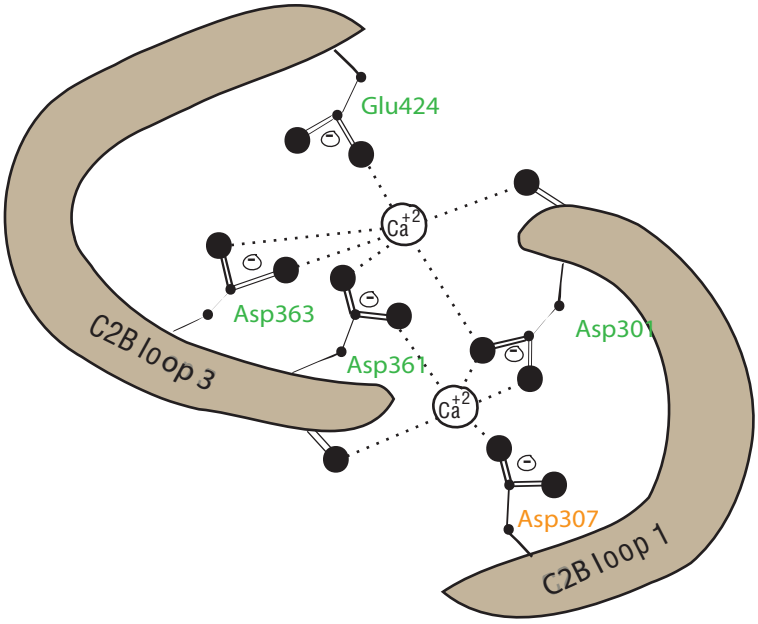

B

```
H. SYT1  M---------- ---------- ---------- ---------- ----VSESHH EALAAPPVTT 17
H. SYT2  M---------- ---------- ---------- ---------- --RNIFKRNQ EPIVAPATTT 19
D. SYT1  MPPNAKSETD AKPEAEPAPA SEPAADLESV DQKLEETHHS KFREVDRQEQ EVLAEKAAEA 60

H. SYT1  VATVLP--SN ATEPASPGEG KED------A FSKLKE--KF MNEL--HKIP LPPWALIAIA 65
H. SYT2  ATMPIGPVDN STESGGAGES QED------M FAKLKE--KL FNEI--NKIP LPPWALIAIA 69
D. SYT1  ASQRIAQVES TTRSATT-EA QESTTTAVPV IKKIEHVGEV VTEVIAERTG LPTWGVVAII 119

H. SYT1  IVAVLLVLTC CFCICKKCLF KKKNKKKGKE KGGKNAINMK DVKDLGKTMK DQALKDDDAE 125
H. SYT2  VVAGLLLLTC CFCICKKCCC KKKKNKKEKG KGMKNAMNMK DMKG-GQD-- -----DDDAE 121
D. SYT1  ILVFLVVFGI IF-FCVRRFL KKRRTKDGKG K---KGVDMK SVQLLGSAYK EKVQPDMEEL 175

H. SYT1  TGLTDGE-EK EEPKEEEKLG KLQYSLDYDF QNNQLLVGII QAAELPALDM GGTSDPYVKV 184
H. SYT2  TGLTEGEGEG EEEKEPENLG KLQFSLDYDF QANQLTVGVL QAAELPALDM GGTSDPYVKV 181
D. SYT1  TENAE-EGDE EDKQSEQKLG RLNFKLEYDF NSNSLAVTVI QAEELPALDM GGTSDPYVKV 234

H. SYT1  FLLPDKKKKF ETKVHRKTLN PVFNEQFTFK -VPYSELGGK TLVMAVYDFD RFSKHDIIGE 243
H. SYT2  FLLPDKKKKY ETKVHRKTLN PAFNETFTFK -VPYQELGGK TLVMAIYDFD RFSKHDIIGE 240
D. SYT1  YLLPDKKKKF ETKVHRKTLS PVFNETFTFK SLPYADAMNK TLVFAIFDFD RFSKHDQIGE 294

H. SYT1  FKVPMNTVDF GHVTEEWRDL QSAEKEE-QE KLGDICFSLR YVPTAGKLTV VILEAKNLKK 302
H. SYT2  VKVPMNTVDL GQPIEEWRDL QGGEKEE-PE KLGDICTSLR YVPTAGKLTV CILEAKNLKK 299
D. SYT1  VKVPLCTIDL AQTIEEWRDL VSVEGEGGQE KLGDICFSLR YVPTAGKLTV VILEAKNLKK 354

H. SYT1  MDVGGLSDPY VKIHLMQNGK RLKKKKTTIK KNTLNPYYNE SFSFEVPFEQ IQKVQVVVTV 362
H. SYT2  MDVGGLSDPY VKIHLMQNGK RLKKKKTTVK KKTLNPYFNE SFSFEIPFEQ IQKVQVVVTV 359
D. SYT1  MDVGGLSDPY VKIAIMQNGK RLKKKKTSIK KCTLNPYYNE SFSFEVPFEQ IQKICLVVTV 414

H. SYT1  LDYDKIGKND AIGKVFVGYN STGAELRHWS DMLANPRRPI AQWHTLQVEE EVDAMLAVKK 422
H. SYT2  LDYDKLGKNE AIGKIFVGSN ATGTELRHWS DMLANPRRPI AQWHSLKPEE EVDALLGKNK 419
D. SYT1  VDYDRIGTSE PIGRCILGCM GTGTELRHWS DMLASPRRPI AQWHTLKDPE ETDEILKNMK 474
```

Figure S1. Conservation of human SYT2 and *Drosophila* SYT1. (**A**) Schematic diagram of the key residues (green) that protrude from the top of the C2B domain that coordinate calcium binding in SYT2 (diagram based on Fernandez *et. al.*[1]). The Asp307 residue is highlighted in orange. (**B**) Alignment of amino acid sequences of human SYT1, human SYT2 and *Drosophila* SYT1, highlighting the conservation between the synaptic vesicle SYT isoforms. The transmembrane domain and the C2A and C2B calcium binding domains are highlighted in black, purple, and blue boxes, respectively. The five key aspartate (D) residues that mediate calcium binding to each C2 domain are indicated with green asterisks. The fifth aspartate reside in C2B in human SYT1 is replaced by a glutamate residue in human SYT2 and *Drosophila* SYT1. The Asp307 residue (Asp362 in *Drosophila*) is shown in the orange box and the Pro308 residue is shown in the pink box.

Figure S2

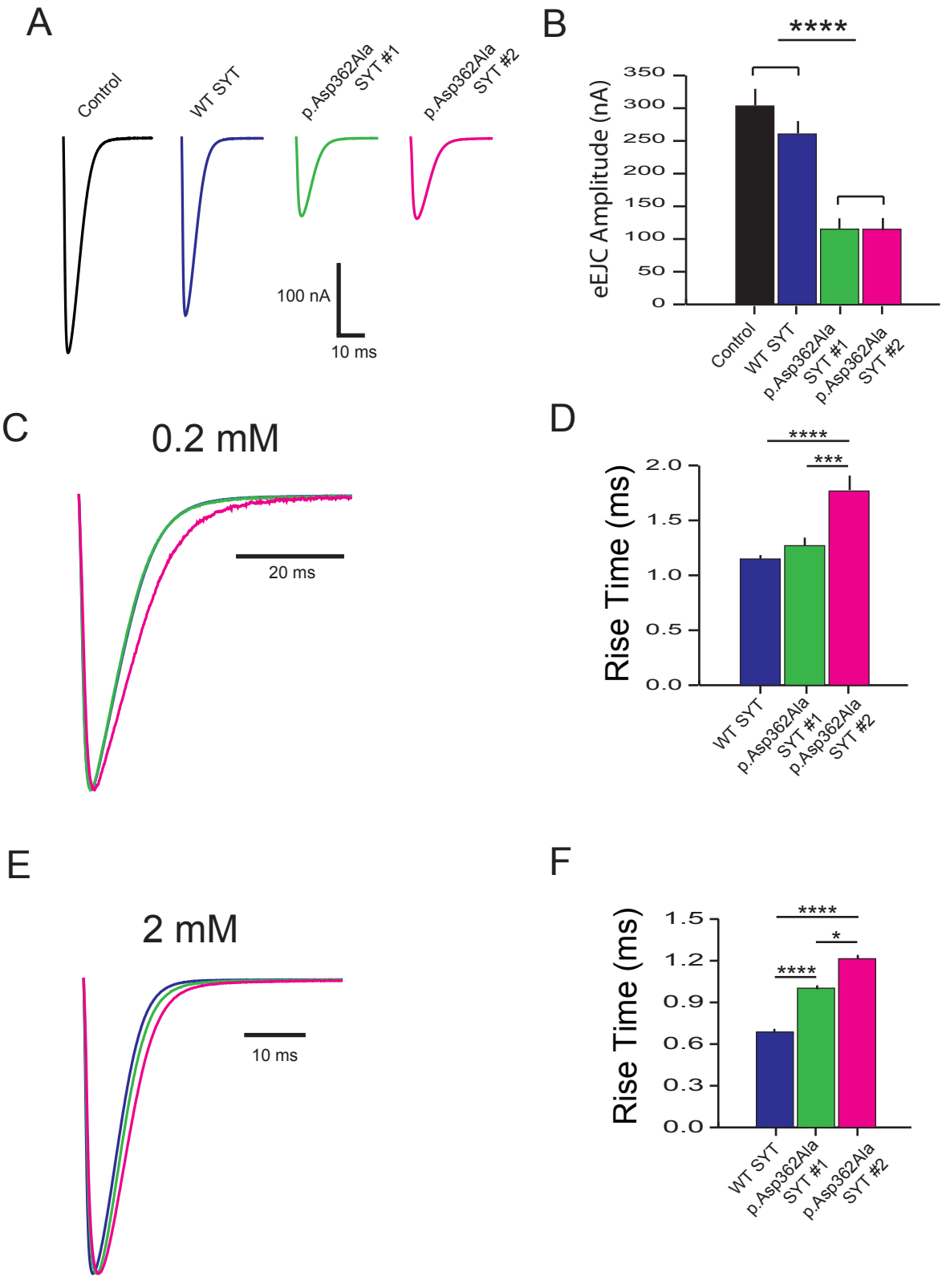
A
Control
WT SYT
p.Asp362Ala SYT #1
p.Asp362Ala SYT #2
100 nA
10 ms
B
****
eEJC Amplitude (nA)
350
300
250
200
150
100
50
0
Control
WT SYT
p.Asp362Ala SYT #1
p.Asp362Ala SYT #2
C
0.2 mM
20 ms
D
****
***
Rise Time (ms)
2.0
1.5
1.0
0.5
0.0
WT SYT
p.Asp362Ala SYT #1
p.Asp362Ala SYT #2
E
2 mM
10 ms
F
****
*
****
Rise Time (ms)
1.5
1.2
0.9
0.6
0.3
0.0
WT SYT
p.Asp362Ala SYT #1
p.Asp362Ala SYT #2

Figure S2. Effects of p.Asp362Ala DSYT1 on synaptic transmission in 0.2 and 2.0 mM extracellular calcium. (**A**) Representative EPSCs recorded in 2.0 mM extracellular calcium at third instar larval muscle 6 synapses for the indicated genotypes (control, WT SYT or p.Asp362Ala DSYT1 in transgenic lines #1 and #2 induced by elav^{C155}-GAL4). Similar to the effects at 0.2 mM calcium, p.Asp362Ala reduces evoked release. (**B**) Quantification of mean eEJC amplitudes in the indicated genotypes ($w^{-/-}$, 303.4±26.4 nA, n=8; elav^{C155}-GAL4; UAS-DSYT1, 260.5±15.7 nA, n=13; elav^{C155}-GAL4; UAS-DSYT1 p.Asp362Ala#1, 115.1±13.1 nA, n=13; elav^{C155}-GAL4; UAS-DSYT1 p.Asp362Ala#2, 114.9±15.7 nA, n=17). (**C**) Average traces of EPSCs normalized to the maximal amplitude following induction of WT DSYT1 (blue), p.Asp362Ala DSYT1#1 (green) or p.Asp362Ala DSYT1#2 (magenta) by elav^{C155}-GAL4 in 0.2 mM external calcium. (**D**) Quantification of average rise time in each genotype. The induction of p.Asp362Ala in transgenic line #2 results in slower kinetics of neurotransmitter release compared to control. Mean rise times at 0.2 mM calcium are: WT DSYT1, 1.15 ± 0.04 ms, n=15; p.Asp362Ala DSYT1#1, 1.27 ± 0.06 ms, n=16; p.Asp362Ala DSYT1#2, 1.77 ± 0.12 ms, n=16. Student's t-test revealed significant differences between WT DSYT1 and p.Asp362Ala DSYT1#2 ($P<0.0002$) and p.Asp362Ala DSYT1#1 and p.Asp362Ala DSYT1#2 ($P<0.002$). (**E**) Average traces of EPSCs normalized to the maximal amplitude following induction of WT DSYT1 (blue), p.Asp362Ala DSYT1#1 (green) or p.Asp362Ala DSYT1#2 (magenta) by elav^{C155}-GAL4 in 2.0 mM external calcium. In higher calcium, both p.Asp362Ala lines have slower rates of release than controls. (**F**) Quantification of average rise time in each genotype. Mean rise times at 2 mM calcium are: WT DSYT1, 0.7 ± 0.03 ms, n=13; p.Asp362Ala DSYT1#1, 1.0 ± 0.05 ms, n=13; p.Asp362Ala DSYT1#2, 1.2 ± 0.06 ms, n=17. Student's t-test revealed significant differences between WT DSYT1 and p.Asp362Ala DSYT1#1 ($P<0.001$),

WT DSYT1 and p.Asp362Ala DSYT1#2 ($P<0.001$) and p.Asp362Ala DSYT1#1 and p.Asp362Ala DSYT1#2 ($P<0.02$).

Figure S3

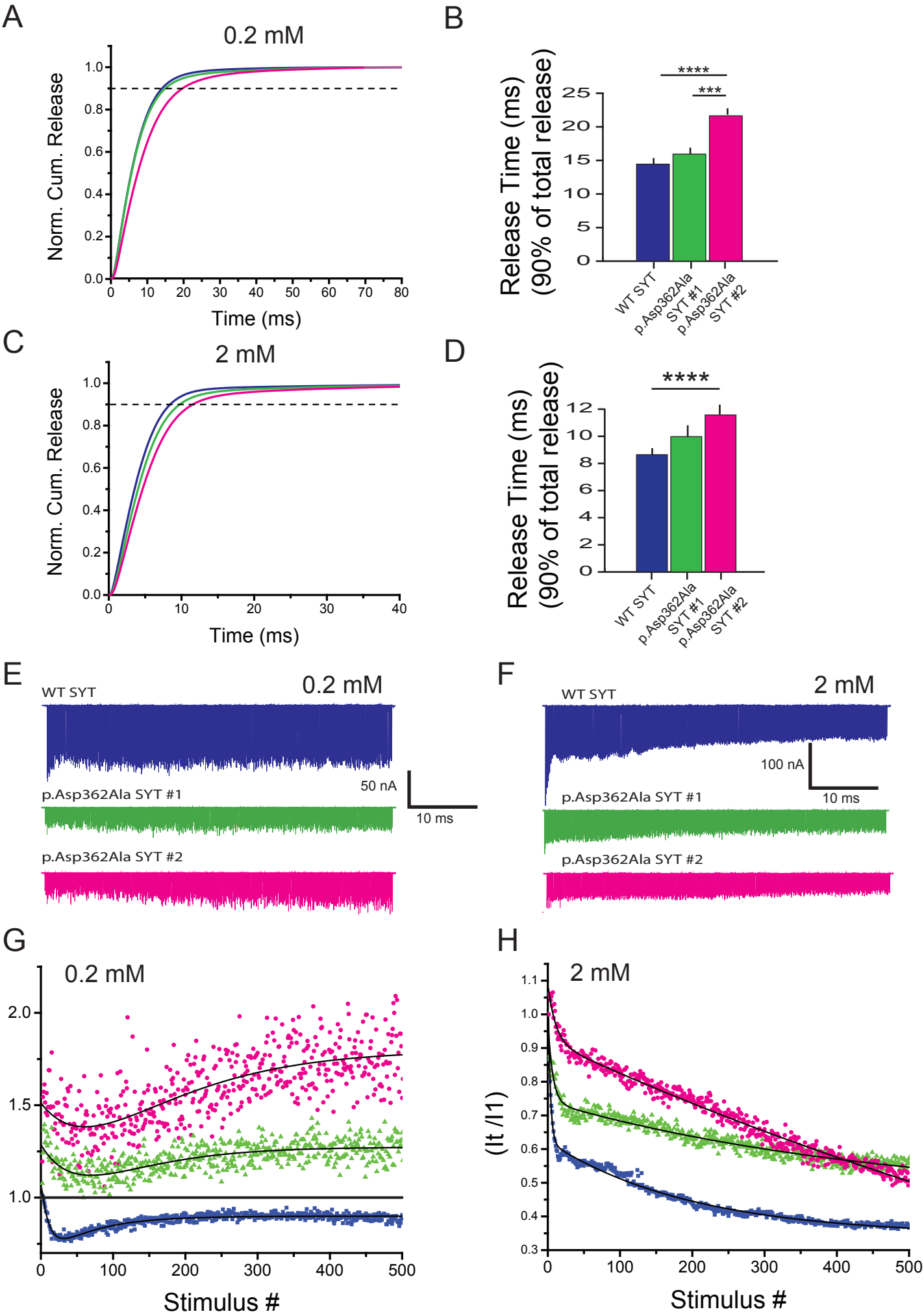
A
0.2 mM
Norm. Cum. Release
Time (ms)
B
Release Time (ms)
(90% of total release)
****
***
WT SYT
p.Asp362Ala SYT #1
p.Asp362Ala SYT #2
C
2 mM
Norm. Cum. Release
Time (ms)
D
Release Time (ms)
(90% of total release)
****
WT SYT
p.Asp362Ala SYT #1
p.Asp362Ala SYT #2
E
WT SYT
0.2 mM
50 nA
10 ms
p.Asp362Ala SYT #1
p.Asp362Ala SYT #2
F
WT SYT
2 mM
100 nA
10 ms
p.Asp362Ala SYT #1
p.Asp362Ala SYT #2
G
0.2 mM
(It / I1)
Stimulus #
H
2 mM
(It /I1)
Stimulus #

Figure S3. Effects of p.Asp362Ala DSYT1 on synaptic transmission kinetics and high frequency stimulation. (**A**) Cumulative response normalized for the maximum following induction of WT DSYT1 (blue), p.Asp362Ala DSYT1#1 (green) or p.Asp362Ala DSYT1#2 (magenta) by elav^{C155}-GAL4 in 0.2 mM external calcium. Dash lines indicate the time at which 90% of the total release has occurred during a single stimulus. Induction of p.Asp362Ala in the transgenic line #2 results in slower rates of release due to an enhancement in the slower asynchronous phase of fusion. (**B**) Quantification of release time when 90% of the total charge was transferred in each condition. Mean release time in the strains at 0.2 mM calcium are: WT DSYT1, 14.4 ± 0.8 ms, n=15; p.Asp362Ala DSYT1#1, 15.9 ± 0.9 ms, n=16; p.Asp362Ala DSYT1#2, 21.6 ± 1.4 ms, n=16. Student's t-test revealed significant differences between WT DSYT1 and p.Asp362Ala DSYT1#2 ($P<0.0001$) and p.Asp362Ala DSYT1#1 and p.Asp362Ala DSYT1#2 ($P<0.005$). (**C**) Cumulative release normalized for the maximum following induction of WT DSYT1 (blue), p.Asp362Ala DSYT1#1 (green) or p.Asp362Ala DSYT1#2 (magenta) by elav^{C155}-GAL4 in 2.0 mM external calcium. Dash lines indicate the time at which 90% of the total release has occurred during a single stimulus. (**D**) Mean release time at 2 mM calcium: WT DSYT1, 8.6 ± 0.4 ms, n=11; p.Asp362Ala DSYT1#1, 10.0 ± 0.8 ms, n=13; p.Asp362Ala DSYT1#2, 11.6 ± 0.7 ms, n=17. Student's t-test revealed significant differences between WT DSYT1 and p.Asp362Ala DSYT1#1 ($P<0.001$). (**E, F**) Representative EPSCs following induction of WT DSYT1 (blue), p.Asp362Ala DSYT1#1 (green) or p.Asp362Ala DSYT1#2 (magenta) by elav^{C155}-GAL4 in 0.2 mM (**E**) or 2.0 mM (**F**) external calcium during 10 Hz tetanic stimulation of the nerve. (**G, H**) Average responses for 500 stimulations normalized to the first response during the tetanus following induction of WT DSYT1 (blue), p.Asp362Ala DSYT1#1 (green) or p.Asp362Ala DSYT1#2 (magenta) by elav^{C155}-GAL4 in 0.2 mM (**G**) or 2.0 mM (**H**)

extracellular calcium. p.Asp362Ala DSYT1 decreases initial release probability and results in facilitation in low calcium (**G**) or slower rates of depression in high calcium (**H**).

Table S1. Electrophysiologic Data (USA1)

Characteristic	I.2	II.2	III.1	III.2
Ulnar motor nerve				
Pre exercise CMAP amp. (mV)	7.3	7.8	4.7	3.3
Post exercise CMAP amp. (mV)	9.3	11.1	9.8	9.9
CV (m/s)	63.6	63.3	61.2	67.8
Median motor nerve				
Pre exercise CMAP amp. (mV)	6.1	4.1	5.5	5.3
Post exercise CMAP amp. (mV)	7.4	9.0	12.0	11.1
CV (m/s)	-	66.6	55.5	61.6
Peroneal motor nerve (TA)				
Pre exercise CMAP amp. (mV)	2.3	1.8	-	-
Post exercise CMAP amp. (mV)	2.9	4.3		
CV (m/s)	50	52.6		
Peroneal motor nerve (EDB)				
Distal CMAP amp. (mV)	0.6	0.3	2.2	-
CV (m/s)	47.2	48.3	62.9	
Tibial motor nerve				
Distal CMAP amp. (mV)	1.5	2.0	-	2.7
CV (m/s)	-	46.4		59
Ulnar sensory nerve				
Amp. (μV)	-	49.6	72.9	27.9
CV (m/s)		51.8	68.7	74.7
Sural sensory nerve				
Amp. (μV)	13.6	16.3	16.2	18.8
CV (m/s)	45.4	68.4	65.2	65.2
Ulnar motor nerve 3Hz RNS				
(% decrement)				
Baseline	0%	10%	4%	22%
Immed. post exercise	-	0%	-	8%

Amp. Amplitude; CMAP Distal compound muscle action potential; CV conduction velocity; TA tibialis anterior muscle; EDB extensor digitorum brevis muscle; RNS repetitive nerve stimulation; - not tested

Table S2. Electrophysiologic Data (UK1)

Characteristic	II.2	III.2		III.7
Ulnar motor nerve				
Pre exercise CMAP amp. (mV)	11.2	4.6		10.6
Post exercise CMAP amp. (mV)	13.5	6.8		13.8
CV (m/s)	60.3	66.7		64
Median motor nerve				
Pre exercise CMAP amp. (mV)	9.4	3.8		8.2
Post exercise CMAP amp. (mV)	11.6	5.8		11.6
CV (m/s)	55.6	56.8		60.6
Peroneal motor nerve (TA)		**R**	**L**	
Pre exercise CMAP amp. (mV)	2.1	1.6	0.5	2.0
Post exercise CMAP amp. (mV)	2.5	5.1	2.6	3.1
Peroneal motor nerve (EDB)				
Distal CMAP amp. (mV)	1.1	0.0		0.9
CV (m/s)	42.0	-		42.9
Tibial motor nerve				
Distal CMAP amp. (mV)	2.8	4.3		-
CV (m/s)	39.5	45.9		-
Ulnar sensory nerve[a]				
Amp. (µV)	12.0	13.0		11.0
CV(m/s)	48.0	57.1		60.1
Sural sensory nerve				
Amp. (µV)	20.0	18.0		31.0
CV (m/s)	45.2	43.7		43.9
Median motor nerve 3Hz RNS (% decrement)				
Baseline	2%	3%		0%

Amp. Amplitude; CMAP Distal compound muscle action potential; CV conduction velocity; TA tibialis anterior muscle; EDB extensor digitorum brevis muscle; RNS repetitive nerve stimulation; [a]orthodromic stimulation; - not tested

Table S3. Whole Exome sequencing in USA1 and UK1: Variants Segregating under an Autosomal Dominant Model with strict filtering and Conservation Criteria.

3a. USA1 Family

CHROMOSOME	POSITION	ALLELE CHANGE	GENE NAME	AMINO ACID CHANGE	SCORE
1	202568479	A>C	SYT2[a]	Asp307Ala	5
2	43809056	C>G	THADA	Gly182Ala	3
2	96798420	C>T	ASTL	Val166Ile	3
8	72234455	G>G	EYA1[a]	Pro84Leu	3
9	131112774	T>C	SLC27A4	Met266Thr	3
15	78836537	T>C	PSMA4	Met72Thr	3

3b. UK1 Family

CHROMOSOME	POSITION	ALLELE CHANGE	GENE NAME	AMINO ACID CHANGE	SCORE
1	202568476	C>T	SYT2[a]	Pro308Leu	5
2	233348883	T>G	ECEL1	His412Pro	3
14	34266771	C>A	NPAS3	Asp438Glu	3

SCORE: This is the composite of 5 protein prediction algorithms where 'damaging' earns one point (Polyphen, Mutation Taster, Mutation Assessor, SIFT, LRT). [a]Variants segregating with disease following Sanger sequencing of all identified genes in USA1 and UK1 families.

Supplemental Reference

1. Fernandez, I., Araç, D., Ubach, J., Gerber, S.H., Shin, O., Gao, Y., Anderson, R.G., Südhof, T.C., Rizo, J. (2001). Three-dimensional structure of the synaptotagmin 1 C2B-domain: synaptotagmin 1 as a phospholipid binding machine. Neuron *32*, 1057-1069 (2001).